

## Application of Inverse Filtering Techniques in the Sea Bottom Recognition

Z. Łubniewski, M. Moszyński, A. Stepnowski

Technical University of Gdańsk, Acoustics Department, ul. Narutowicza 11/12, 80-952 Gdańsk, POLAND  
e-mail: lubniew@eti.pg.gda.pl

*The paper presents the newly developed approach to the sea bottom recognition and identification, which uses inverse filtering techniques to extract bottom scattering properties from a single-beam echosounder signal. Using simple physical model, the developed inverting procedure allows to remove the influence of pulse shape, beam pattern and model geometry upon the backscattered echo. It permits to obtain the seabed impulse response which is directly related to the function describing the angular dependence of bottom reverberation coefficient. Various direct and iterative inverse methods can be applied to the mentioned problem. The results of testing the method using echoes from several bottom types are in agreement with the predictions of theoretical models. Moreover, the proposed bottom classification procedure uses simple parameters of deconvolved function and the obtained classification results are better than those of other bottom identification methods of normal incidence.*

### 1. Introduction

Acoustic methods of bottom characterisation have known advantages, as they are non-invasive and more cost effective than other methods, e. g. using geological cores. The methods of so called normal incidence – which use the backscatter data from a single-beam echosounder – have achieved special attention, due to their simplicity, accessibility and versatility. They can involve several approaches such as:

- measurement of energy ratio of the first and second bottom echo [2],
- comparison of theoretically modelled and measured echo patterns [1], [7], [10],
- analysis of a set parameters of the echo envelope using cluster analysis [3], artificial neural networks [6], [9] or fuzzy logic [6],
- evaluating the fractal dimension of echo envelope [4] or deconvolved bottom impulse response [5].

The authors propose the novel approach to the sea bottom identification, which uses the newly developed inverse filtering techniques, previously successfully applied to the indirect *in-situ* fish target strength estimation [8]. Assuming the simple physical model of surface scattering of acoustic signal on the seabed, application of the inverse filtering allows to remove the influence of sounding pulse shape, beam pattern, propagation loss and model geometry upon the received single-beam echosounder echo. As a result we obtain the information about bottom spatial scattering properties expressed in an angular variability of its surface reverberation coefficient, what may be then used in the bottom type classification.

### 2. Formulation of the problem

Consider the echosounder signal with pressure time dependence

$$p(t) = p_e(t) \cdot \cos(2\pi f_0 t), \quad (1)$$

where  $f_0$  is the carrier frequency and  $p_e(t)$  is the envelope. The transmit/receive beam pattern is assumed to be  $b(\psi, \varphi) = b(\varphi)$ , where  $\psi \in (0^\circ, 360^\circ)$  - azimuth angle,  $\varphi \in (0^\circ, 90^\circ)$  - incident angle. The signal is emitted vertically downward the sea bottom and beam pattern does not depend on the azimuth angle  $\psi$ . Due to high operating frequency of echosounder (120 kHz), the signal is believed to be scattered only on bottom surface and the volume scattering effects are neglected. To derive the expressions relating received echo envelope to the angular dependence of bottom backscattering coefficient as well as the sounding pulse shape and beampattern, the authors used the simplified version of model described in [7] and assumed:

- the absence of the large scale bottom roughness, what means that bottom relief is small compared with the model geometry, so the bottom may be treated as approximately flat,

- the domination of noncoherent component in backscattered signal,

- the attenuation coefficient in water  $\alpha = 0$  and the absence of refraction in water column.

Under the assumption of a scattered signal noncoherence, the received echo intensity is the sum of echo intensities from all infinitesimal scattering elements  $dS$  of insonified bottom surface area  $S$ . The echo from a given scattering element  $dS$  must be weighted by squared beampattern  $b^2(\varphi)$  and spherical spreading loss factor  $\frac{1}{R^4}$ , where  $R$  is the distance from transducer to  $dS$ .

The transmitted echo intensity is proportional to its squared pressure envelope  $p_e^2$  and the received echo intensity is proportional to the received squared pressure envelope (varying slowly in time) with the same coefficient of proportionality. Then, if  $p_e^2$  is constant during entire sounding pulse, the squared echo envelope denoted by  $\nu(t)$ , may be expressed by integral [7]:

$$\nu(t) = p_e^2 \iint_S \frac{1}{R^4} b^2(\varphi) s_s(\varphi) dS, \quad (2)$$

where  $s_s(\varphi)$  is the bottom surface reverberation coefficient for  $\varphi$  as an angle of incidence and scattering, defined as a ratio:

$$s_s(\varphi) = \frac{I_s}{I_0}, \quad (3)$$

where  $I_0$  is the incident wave intensity and  $I_s$  the scattered wave intensity measured at the unit distance from the unit scattering surface.

To obtain the scattering impulse response of the bottom, it was more convenient to derive first the bottom unit response and then use it to obtain the impulse response. Assume that the emitted signal envelope has the shape of Heaviside unit step:

$$1(t) = \begin{cases} 1 & \text{for } t \geq t_0 \\ 0 & \text{for } t < t_0 \end{cases} \quad (4)$$

rather than the Dirac delta pulse  $\delta(t)$ . In the case of unit step, where  $p_e^2 = 1$  for whole semi-axis of  $t \geq t_0$ , the squared echo envelope  $h(t)$  is:

$$h(t) = \iint_S \frac{1}{R^4} b^2(\varphi) s_s(\varphi) dS. \quad (5)$$

In this case, at a given moment  $t$  an echosounder insonifies the bottom area of the shape of a circle with radius  $\rho_{max}(t)$ , while in the case of Dirac pulse only the arc of this circle would be insonified (see Fig. 1 for comparison of  $1(t)$  and  $\delta(t)$  signal spreading and Fig. 2 for geometry of the problem). The radius  $\rho_{max}$  is

$$\rho_{max} = \sqrt{R_{max}^2(t) - H^2}, \quad (6)$$

where  $H$  is bottom depth and the distance  $R_{max}$  is related to the time  $t$  from the beginning of the echo by

$$R_{max} = H + \frac{ct}{2}, \quad (7)$$

where  $c$  - the sound speed in water.

Substituting the double integral in (5) by iterative integration in polar co-ordinates  $(\rho, \psi)$ , where  $dS = \rho d\rho d\psi$ , we obtain:

$$h(t) = \int_0^{2\pi} \left( \int_0^{\rho_{max}(t)} \frac{1}{R^4} b^2(\varphi) m_s(\varphi) \rho d\rho \right) d\psi. \quad (8)$$

The distance  $R$  from the transducer to the scattering element  $dS$  is related to the time  $t$  from the beginning of echo by  $R = H + \frac{ct}{2}$ , and the distance  $\rho$  from element  $dS$  to the scattering circle center is

$$\rho = \sqrt{R^2 - H^2} = \sqrt{cHt + \frac{c^2 t^2}{4}}. \quad (9)$$

Including the above relations for substitution of  $\rho$  by time and integrating along  $\psi$  yields

$$h(t) = \pi c \int_0^t b^2(\varphi) s_s(\varphi) \left( H + \frac{c\tau}{2} \right)^{-3} d\tau. \quad (10)$$

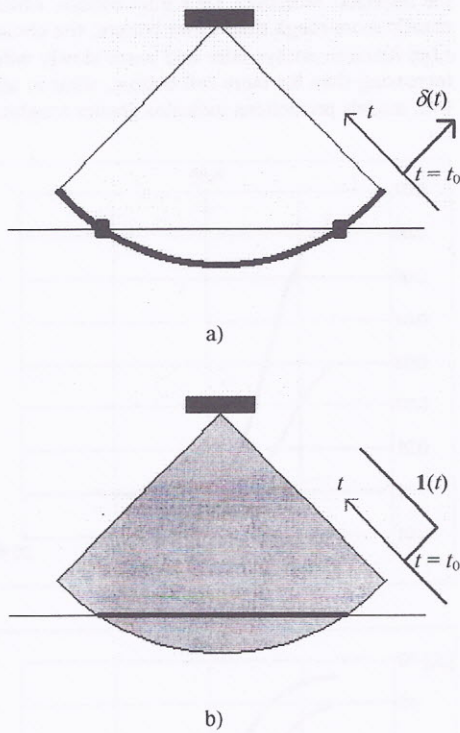


Fig. 1. Vertical cross-sections of water column and parts of flat bottom (boldfaced) insonified by sounding signals in the case of: a) delta pulse  $\delta(t)$ : an arc in water column and two points on line representing bottom, b) unit step  $1(t)$ : circular sector in water column and segment on line representing bottom

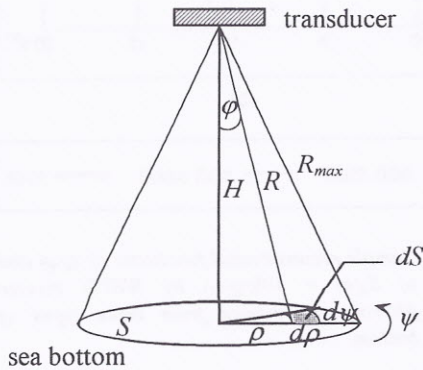


Fig. 2. The geometry of the problem.

Because of the assumption of the approximately flat bottom, the incident angle  $\varphi$  for a wave ray scattered on a given surface element  $dS$  is strictly related to the time of its echo return by:

$$\varphi(t) = \arccos \frac{H}{H + \frac{ct}{2}} \quad (11)$$

and therefore  $b^2$  and  $s_s$  functions may also be treated as functions of time. To obtain the impulse response  $k(t)$  of considered system, we have to differentiate the eq. (10) with respect to time:

$$\begin{aligned} k(t) &= \frac{dh(t)}{dt} = \\ &= \pi c b^2 [\varphi(t)] s_s [\varphi(t)] \left( H + \frac{ct}{2} \right)^{-3} \end{aligned} \quad (12)$$

Now let us denote the known function  $\pi c b^2 [\varphi(t)] s_s [\varphi(t)] \left( H + \frac{ct}{2} \right)^{-3}$  by  $w(t)$ . Then

$$k(t) = w(t) s_s [\varphi(t)] \quad (13)$$

and the system response for arbitrary given input signal with squared envelope denoted by  $x(t)$  is given by convolution integral:

$$\begin{aligned} y(t) &= x(t) * k(t) = \\ &= \int_{-\infty}^{+\infty} w(\tau) s_s [\varphi(\tau)] x(t - \tau) d\tau \end{aligned} \quad (14)$$

Assuming pulse and echo shape  $x(t)$  and  $y(t)$  as well as  $w(t)$  function to be known, the unknown function  $s_s(\varphi)$  describing bottom scattering properties, may be obtained by deconvolution (in time domain) or using inverse filtering procedure (in frequency domain).

### 3. Windowed Singular Value Decomposition

The solution of the considered problem can be obtained by application of both direct inverse methods: Windowed SVD, Regularisation, Wavelet-Waguelette Transform, and iterative methods: Maximum Entropy, Expectation-Maximisation-Smoothing [8]. In this first approach, the authors have chosen the Windowed SVD method.

Assuming finite length of all functions in (14) and discretising the time domain, functions  $x(t)$ ,  $y(t)$ ,  $w(t)$  and  $s_s[\varphi(t)]$  may be substituted by vectors:  $\mathbf{x} = [x_1, \dots, x_M]^T$ ,  $\mathbf{y} = [y_1, \dots, y_{M+N-1}]^T$ ,  $\mathbf{w} = [w_1, \dots, w_N]$ ,  $\mathbf{s} = [s_1, \dots, s_M]^T$ . Then the equation (14) may be written in matrix form:

$$\mathbf{y} = \mathbf{Xs}, \quad (15)$$

where  $X$  is the kernel matrix constructed as follows:

$$X = \begin{bmatrix} x_1 w_1 & & & & 0 \\ x_2 w_1 & x_1 w_2 & & & \\ \dots & x_2 w_2 & x_1 w_3 & & \\ x_M w_1 & \dots & x_2 w_3 & \dots & \\ & x_M w_2 & \dots & \dots & x_1 w_N \\ & & x_M w_3 & \dots & x_2 w_N \\ & & & \dots & \dots \\ 0 & & & & x_M w_N \end{bmatrix} \quad (16)$$

The solution  $s$  may be obtained by pseudo-inverting of matrix  $X$  by WSVD algorithm:

$$\begin{aligned} X &= US_x V^T = [U] \text{diag}(S_{x_i}) [V^T] \\ X^\# &= US_x^{-1} V^T = [U] \text{diag}(1/S_{x_i}) [V^T] \end{aligned} \quad (17)$$

where the matrices  $U$  and  $V$  are orthonormal and their columns are the left and right singular vectors of  $X$  respectively, and the diagonal matrix  $S_x$  represents the singular values  $S_{x_i}$  of matrix  $X$  in non-increasing order.

Because the problem is ill-posed, it was necessary to introduce weights  $W_i$  to prevent the solution from being unstable due to division by small singular values of  $X$ :

$$X^\# = US_x^{-1} V^T = [U] \text{diag}(W_i / S_{x_i}) [V^T]. \quad (18)$$

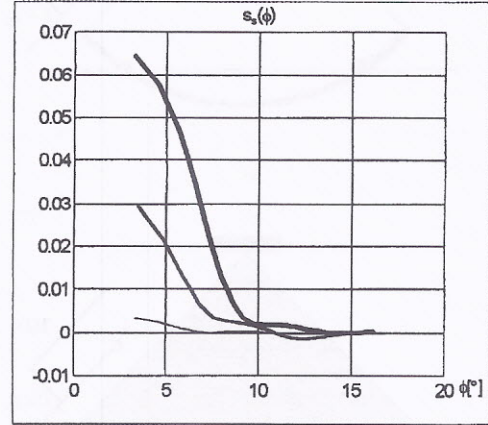
The simple selection of weights in WSVD was used in the form of truncation:  $W_i = 0$  for these singular values  $S_{x_i}$ , which are less than the greatest singular value  $S_{x_1}$  multiplied by 0.001,  $W_i = 1$  for the others.

#### 4. Results

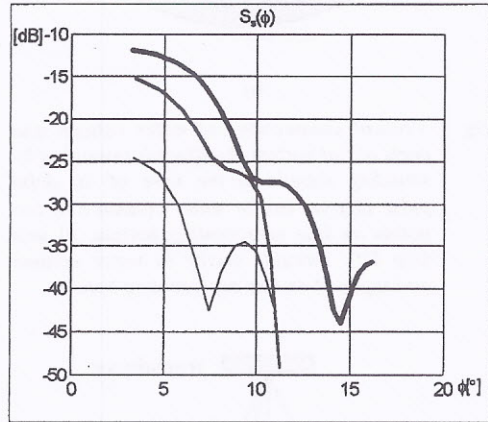
Fig. 3 shows the comparison of the sample results of backscattering coefficient  $s_s(\varphi)$  and its logarithmic equivalent - surface backscattering strength  $S_s = 10\log(s_s)$  reconstruction by inverse filtering applied for acoustic echoes from three different types of bottom: soft mud, soft sand and rock. The data were acquired on Lake Washington with the use of the digital DT4000 echosounder with operating frequency 120 kHz, pulse length 0.4 ms and sampling frequency 41.66 kHz. In order to decrease the influence of random effects (generated by vessel's pitching and rolling), the packages of 10 consecutive echoes were averaged prior to the inverse procedure applying.

There are visible differences between inverted  $s_s(\varphi)$  and  $S_s(\varphi)$  functions for particular sea bottom types, as well as their agreement with models predictions [7], at least in their main,

decaying part. For harder bottom, the inverted  $s_s$  functions have greater values, especially near the angle of normal incidence, where  $s_s$  coefficient is positively related to reflection coefficient for ideally flat interface. Moreover, for harder bottom, which is usually more rough than softer bottom, the obtained  $s_s(\varphi)$  function decays later and more slowly with  $\varphi$  increasing than for more soft bottom, what in agree with models predictions indicates greater roughness.



a)



b)

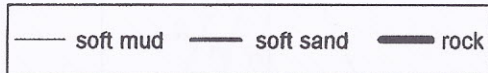


Fig. 3. Sample reconstructed functions: a)  $s_s(\varphi)$  and b)  $S_s(\varphi) = 10\log(s_s)$  by WSVD inverse filtering for echoes from three types of bottom.

Some oscillations of obtained functions within regions of their lower values for greater incident

angles are probably due to periodic (Fourier-type) character of eigenfunctions used in SVD decomposition method. This method does not also guarantee that inverted function would have only non-negative values, specially in regions where it is close to zero.

In addition, the bottom classification procedure based on two parameters of inverted backscattering strength function  $S_s(\varphi)$ , was proposed and tested by constructing the  $2^D$  plots of these parameters values distributions for particular bottom types. The first parameter was defined as the mean slope of the main, decaying part of backscattering strength function:

$$P_1 = a, \quad (19)$$

where  $a$  is the slope of the best fit line for the region of  $\varphi \in (3^\circ, 8^\circ)$  of  $S_s(\varphi)$  in a sense of a minimum mean-square error. Referring to models mentioned in [7], it may be treated as the bottom roughness indicator.

The second parameter was defined as the  $s_s$  coefficient value for the angle nearest zero:

$$P_2 = s_s(\text{first sample}) \quad (20)$$

as bottom hardness indicator related to the flat interface reflection coefficient.

The plots of  $P_1$  and  $P_2$  parameters distributions were constructed both for all echoes in the dataset and for selected 20% echoes with the highest maximal amplitude level believed to return from the most normal incidence of sounding pulse, in order to investigate and remove the influence of the ship's pitching and rolling during the data acquisition. The Fig. 4a contains the  $2^D$  plot of  $P_1$  and  $P_2$  for echoes from entire dataset and Fig. 4b contains the  $P_1$  and  $P_2$  distribution for selected 20% echoes with the highest maximal amplitude.

It is easily seen from both parts of Fig. 4, that obtained  $P_1$  and  $P_2$  values for particular types of bottom are consistent with expectations. In general, harder bottom has greater values of hardness as well as roughness indicator. The particular bottom classes are very well separable in the case of 20% echoes with the highest amplitude.

Echoes from muddy bottom have significantly different  $P_1$  as well as  $P_2$  values than echoes from sandy and rocky bottom. However, while classes of rock and sand are well separable on the basis of  $P_2$  parameter, they have quite similar distributions of  $P_1$ . It may be related to the fact, that in absolute domain, echo envelopes from rocky and sandy bottom do not differ much from each other in a sense of time domain primary features, like echo main part length. The applied WSVD method,

which gives the results smoothed by applying the truncation of singular kernel matrix values, is not very sensitive to the small scale features of investigated echo envelopes.

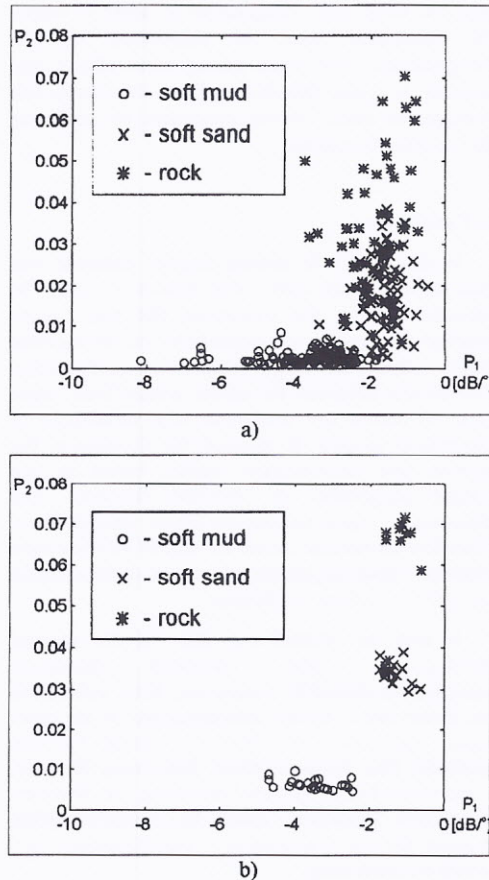


Fig. 4. The obtained  $2^D$  plots of parameters:  $P_1 =$  slope of the best line fit for the region of  $\varphi \in (3^\circ, 8^\circ)$  of  $S_s(\varphi)$  function and  $P_2 = s_s(\text{first sample})$  values distributions for particular 3 types of bottom: a) for echoes from entire dataset, b) for selected 20% echoes with the highest amplitude level.

In the case of all echoes in dataset, the  $P_1$  and  $P_2$  parameters have more wide distributions and echoes from rocky and sandy bottom are partially confused. It seems to be the result of ships' pitching and rolling, what caused the deviation of sounding pulse direction from normal to the bottom and influenced the returning echo level.

In the end, it must be pointed out, that simplicity of presented model assumptions involves the

necessity of care in the results interpretation. In reality, the inverted  $s_r(\varphi)$  function need not be  $s_r$  itself. It may be the sum of  $s_r$  and volume scattering coefficient  $s_v$ , or it may be the convolution of this angular dependence of reverberation coefficient with the large scale distribution of depth  $H$  within the insonified area, as mentioned in [7]. Nevertheless, even when taking these effects into account, it is also possible to draw some important conclusions about bottom properties by analysing the inverted functions.

## 5. Conclusions

In this work, the bottom impulse response was derived in simple form, what allows to apply the inverse filtering for extracting the sea bottom reverberation coefficient dependence on the incident angle - from the single-beam echosounder echo. The results obtained for actual echoes from three types of bottom are consistent with predictions of theoretical models. It allowed for developing the bottom type identification method based on two simple parameters of inverted function. The obtained  $2^D$  plots' results are better than those of other known normal incidence seabed identification methods. However, the larger amount of data should be used for method verification.

It may be pointed out, that in the method development, more advanced theoretical assumptions should be considered, both, referred to the model and to results interpretation. On the other hand, application of different inverse filtering methods, like Regularisation, Maximum Entropy, Expectation-Maximisation-Smoothing or Wavelet-Waguelette Transform, should be considered. What is more, the use of wideband or multifrequency data would be interesting.

## Reference

- [1] A. Caiti, R. Zoppoli, Seafloor parameters identification from parametric sonar data, Proceedings of the 4<sup>th</sup> European Symposium on Underwater Acoustics, Rome, pp. 307-312, (1998).
- [2] R. C. Chivers, N. Emerson, D. R. Burns, New acoustic processing for underway surveying, The Hydrographic Journal 56, pp. 8-17, (1990).
- [3] Z. Klusek, A. Śliwiński, J. Tęgowski, Characteristic properties of bottom backscattering in the South Baltic Sea, Proceedings of the 2<sup>nd</sup> European Conference on Underwater Acoustics, Copenhagen, pp. 105-110, (1994).
- [4] Z. Łubniewski, A. Stepnowski, Application of the fractal analysis in the sea bottom recognition, Archives of Acoustics 23, 4, pp. 499-511, (1998).
- [5] Z. Łubniewski, A. Stepnowski, Sea bottom recognition using fractal analysis and scattering impulse response, Proceedings of the 4<sup>th</sup> European Conference on Underwater Acoustics, Rome, pp. 179-184, (1998).
- [6] J. Maciulowska, A. Stepnowski, T. V. Dung, Fish schools and seabed identification using neural networks and fuzzy logic classifiers, Proceedings of the 4<sup>th</sup> European Conference on Underwater Acoustics, Rome, pp. 275-280, (1998).
- [7] E. Pouliquen, X. Lurton, Identification de la nature des fonds marins à l'aide de signaux d'écho-sondeurs - I. Modélisation des échos réverbérés par le fond, Acta Acustica 2(1), pp. 113-126, (1994).
- [8] A. Stepnowski, Comparison of the novel inverse techniques for fish target strength estimation [invited paper], Proceedings of the 4<sup>th</sup> European Conference on Underwater Acoustics, Rome, pp. 187-192, (1998).
- [9] A. Stepnowski, M. Moszyński, R. Komendarczyk, J. Burczyński, Visual real-time Bottom Typing System (VBTS) and neural networks experiment for sea bed classification, Proceedings of the 3<sup>rd</sup> European Conference on Underwater Acoustics, Heraklion, pp. 685-690, (1996).
- [10] D. D. Sternlicht, C. de Moustier, Temporal modelling of high frequency (30 - 100 kHz) acoustic seafloor backscatter: shallow water results, Saclantcen Conference Proceedings Series CP-45, High Frequency Acoustics in Shallow Water, La Spezia, pp. 509-516, (1997).